

Performance Evaluation of Wind Turbine Generators under System Fault Conditions in a Multi-Machine Power System

Chintan R. Mehta, Urmil B. Bhatt, Dishang D. Trivedi, Santosh C. Vora

Abstract: *The electrical power generation is augmented by the deployment of renewable energy sources apart from the conventional synchronous generators (SGs). Wind energy, one of the extensively extracted renewable resource is mainly derived using induction generators (IGs). The IGs have different electrical performance characteristics depending on its type and hence their behaviour under faulty conditions are quite different as compared to synchronous generators. Researchers have proposed the peak current contribution of IGs during various faults at point of common coupling (PCC) with single machine infinite bus (SMIB). This paper presents performance evaluation of different types of IGs operating with SGs in a multi-machine power system by considering a high penetration of wind energy. The reactance diagram of multi-machine power system is deliberated. A three L-G fault is simulated at weak bus of the system and results are presented and analysed for various wind turbine generators.*

Index Terms: *Induction generators, multi-machine system, reactance diagram, short circuit current, wind energy*

I. INTRODUCTION

The non-depleting resources and the enabling technologies are the areas of thrust to fulfill the energy needs of the mankind and address environment concerns. The challenges associated with the renewable energy sources like intermittency, limited resource extraction capacity, asynchronous operation, lower efficiency etc., demands for many technological considerations while using them in conjunction with conventional power generators. The solar and wind energy generation technologies have matured to answer some of the above challenges and investigations are on for further improvements. The wind based generation, trending in renewable generation until now, offers a good flexibility in wind energy extraction. Various types of asynchronous wind generators and associated power electronic converters (in certain types) make them suitable for quick integration in conventional system. Considering variety of IGs, their operating state and converter controls, it becomes essential to study their behaviour under steady and

transient conditions of the grid. The current contribution by the IGs and SGs in the event of system faults vary according to the instance, location, pre-fault conditions, voltage profile and loading on the system. For such cases, the relaying systems should be able to discriminate faults and the circuit breakers shall be able to disconnect the system while facilitating fault energy dissipation.

The synchronous generators are equipped with independent field winding which control the flux during the transient events. As the flux is independent of grid voltage, calculation of short circuit current is straight forward. Moreover the rotational speed is fixed and it has no slip like IGs. However, in case of asynchronous generators (IGs) flux being dependent on the grid voltage makes the calculation of short circuit current a bit complex and the standard IEC 60909 is not directly applicable [1]. The fault current of IGs does not persist after finite time due to unavailability of flux in the event of terminal faults. The trapped flux diminishes based on IGs time constant [2]. The short circuit current analysis of various types of wind turbine generators is proposed in [3] for terminal faults for single machine infinite bus (SMIB) system. The paper addresses the difficulties that distance or over current relays can experience when they are used with different types of wind turbines. Analytical method for calculating the short circuit current is proposed in [4]. The effect of different fault types i.e. symmetrical faults and asymmetrical faults, transformer configuration and reactive power compensation capacitors on different IGs have been shown in [5]. The short circuit current contributions of different IGs for generator terminal faults are simulated using time domain simulations and steady-state calculations in [6]. The authors have proposed a method to calculate the short circuit current for SMIB and the results have been compared

with the commercial software. The short circuit modelling of various types of wind power plants for symmetrical and asymmetrical faults for SMIB have been proposed by the authors of [7]. The differences between a crowbar-protected doubly fed induction generator and conventional induction generator is highlighted and approximate equations for the maximum short-circuit current of a doubly fed induction generator are proposed in [8]. The detailed analysis of the negative sequence current response under various control objectives for unbalanced grid fault by considering various controller parameters for SMIB is proposed by [9]. The effects of wind speed variation on the fault current level of the wind turbine generators and its protection settings is shown in [10].

Revised Manuscript Received on March 08, 2019.

Chintan R. Mehta, (Corresponding author) Electrical Engineering Department, Institute of Technology, Nirma University, Ahmedabad, India.

Urmil B. Bhatt, Electrical Engineering Department, Institute of Technology, Nirma University, Ahmedabad, India.

Dishang D. Trivedi, Electrical Engineering Department, L.D. College of Engineering, Ahmedabad, India.

Santosh C. Vora, Electrical Engineering Department, Institute of Technology, Nirma University, Ahmedabad, India.

Analytical derivation for short circuit current of DFIG by considering closed loop transfer functions have been proposed and validated for SMIB in [11]. The control strategy to re-establish the terminal voltage of wind turbine after the clearance of fault is proposed by [12]. Phasor domain based short circuit model for protection applications of DFIG is proposed by [13]. To determine transient stability, P - δ curve is used in case of synchronous generator. The analogy with respect to torque-speed characteristic is proposed for IGs. The study on short circuit current of DFIG, with attention to the transfer of negative-sequence voltage in the rotor-side converter is proposed in [14]. The authors of [15] have shown effects of the power electronic converters of DFIG wind farms and concluded that it helps to maintain transient stability of the system when connected with SG. The review of protection schemes for renewable integrated power networks in transmission and distribution systems is proposed in [16]. Authors of [17][18] have shown line protection challenges experienced in system having substantial wind energy penetration. The authors of [19] have shown the effect of fault location on power swing and fault current contribution of DFIG based wind farm in large power system.

The literature survey mostly highlights the results of deploying induction generator in single machine infinite bus (SMIB) system, where the short circuit at the generator terminal is simulated and the observations are neatly depicted. This research work focuses on the performance evaluation of various types of wind turbine generators especially induction based generators under the system fault conditions in a multi-machine power system. The authors have considered western system coordinating council (WSCC) 3 generator 9 bus system for analyzing the effect of fault at system level. The authors have deliberated the reactance diagram of WSCC 9 bus system. The reactance diagram with slight modification can be used to identify the peak short circuit current when the conventional SG is replaced by various types of IGs. The knowledge of peak short circuit current will help of the system operator to decide the changes in relay and circuit breaker setting at the time of system level faults under the high penetration of IGs.

II. SHORT CIRCUIT CURRENT CALCULATION FOR AN INDUCTION GENERATOR

The equivalent circuit of an induction machine is given by [8] is shown in Figure 1. For the analysis of induction machine state vector description is used. In synchronously rotating reference frame, the equations describing an induction machine are given by [8].

In (1) and (2) $\vec{\Psi}_s$ and $\vec{\Psi}_r$ term represents flux linkages of stator and rotor respectively. (3) and (4) represents stator voltage imposed by the grid and rotor voltage controlled by the rotor side converter and it is used to perform the generator control.

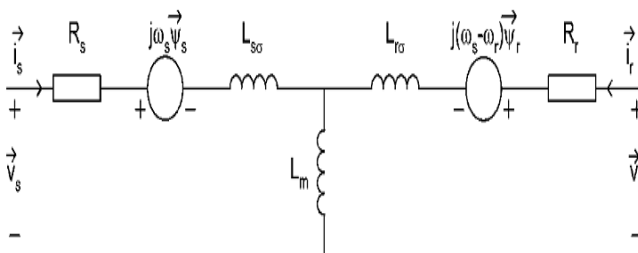


Figure 1: Equivalent circuit of an induction machine for transient analysis

$$\vec{\Psi}_s = L_s \vec{i}_s + L_m \vec{i}_r \quad (1)$$

$$\vec{\Psi}_r = L_r \vec{i}_r + L_m \vec{i}_s \quad (2)$$

$$\vec{v}_s = R_s \vec{i}_s + \frac{d\vec{\Psi}_s}{dt} + j\omega_s \vec{\Psi}_s \quad (3)$$

$$\vec{v}_r = R_r \vec{i}_r + \frac{d\vec{\Psi}_r}{dt} + j(\omega_s - \omega_r) \vec{\Psi}_r \quad (4)$$

Here ω_s and ω_r represents stator and rotor angular speed respectively. R_s and R_r represents stator resistance and rotor resistance respectively. L_s is stator inductance, L_r is rotor inductance and they are related to the stator leakage inductance $L_{s\sigma}$ and the rotor leakage inductance $L_{r\sigma}$ according to the following expressions:

$$L_s = L_{s\sigma} + L_m, \quad L_r = L_{r\sigma} + L_m \quad (5)$$

Where L_m is magnetizing inductance.

σ is the leakage co-efficient of machine and is given by $[1 - (L_m^2 / L_s L_r)]$.

The transient stator inductance and transient rotor inductance can be written as

$$L'_s = L_{s\sigma} + \frac{L_{r\sigma} L_m}{L_{r\sigma} + L_m} \quad (6)$$

$$L'_r = L_{r\sigma} + \frac{L_{s\sigma} L_m}{L_{s\sigma} + L_m} \quad (7)$$

The damping of the SC current is governed by the time constant of the induction generator and they are given by

$$T'_s = \text{stator transient time constant} = L'_s / R_s$$

$$T'_r = \text{rotor transient time constant} = L'_r / R_r$$

X'_s = impedance seen by machine at time of fault.

The stator and rotor coupling factors can be known as

$$k_s = \frac{L_m}{L_s}, \quad k_r = \frac{L_m}{L_r} \quad (8)$$

by considering the above parameters, the stator and rotor current can be considered as in [8]

$$\vec{i}_s = \frac{1}{L'_s} [\vec{\Psi}_s - k_s \vec{\Psi}_r] \quad (9)$$

$$\vec{i}_r = \frac{1}{L'_r} [\vec{\Psi}_r - k_s \vec{\Psi}_s] \quad (10)$$

The maximum value of short circuit current of an induction machine is given by [5][8]

$$i_{sc,max} = \frac{\sqrt{2}V_s}{X'_s} [e^{-T/2T'_s} + (1 - \sigma)e^{-T/2T'_r}] \quad (11)$$

The envelop of SC current for different types of generators are different and are dependent on the time constant of the machine. The time constant of Type II (WRIG) and Type III (DFIG) generators is lower as compared to Type-I

(FSIG) generators because of presence of rotor resistance in both the machines.

At the time of symmetrical faults, the crowbar is activated for the protection of converters in DFIG and the DFIG acts as simple induction generator but with the practical differences introduced by different pre-fault conditions. FSIG and WRIG generators operates at very low slip but DFIG operates with large slip, which will create significant rotor current induced frequency components in stator winding, producing sinusoidal fault current contributions that are not at fundamental frequency. (11) comprises of two terms i.e. a DC component and a steady state component. DC component term will die out based on stator time constant. Unlike synchronous generator, second term is having $e^{-T/2T'r}$ term. This term will also die out after finite time constant which depends on rotor circuit. This decay nature of current will also bring change in fault response of other machines feeding same fault. Due to non-availability of excitation in IGs, the voltage at bus will ramp down to zero. Thus it will also change the voltage profile of the other SGs present in the system which will eventually change the reactive power output of other conventional SGs.

III. SYSTEM DESCRIPTION

The WSCC test system comprises of three synchronous generators, nine buses and loads as shown in Figure 2 [20].

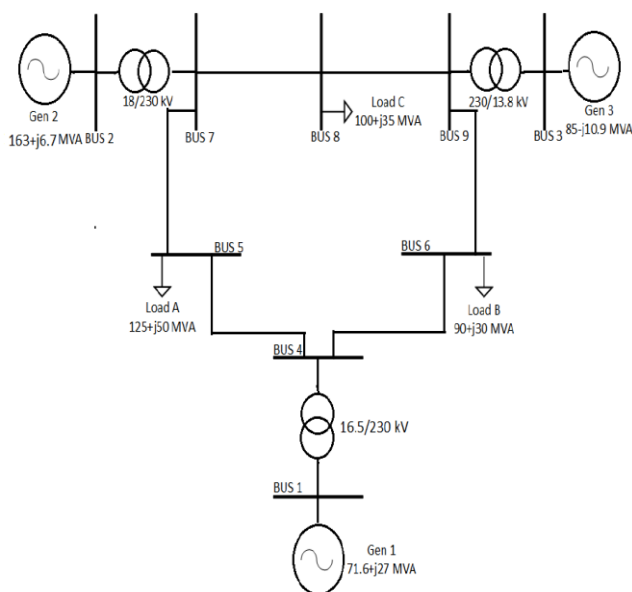


Figure 2: A WSCC 3-generator 9-Bus Test System

In this system, a synchronous generator at bus 2 is replaced by its equivalent capacity wind turbine generators of FSIG, WRIG and DFIG based wind farms. The total demand of WSCC system is 315 MVA and the wind farm capacity is 192 MVA which shows high penetration of wind energy. The other generators and the loads are as per the standard test system specifications. The entire wind farm operating at wind velocity of 11 m/s. The steady state operation of the modified system is same as the conventional system. To analyze the performance of the system, a symmetrical fault at the bus 5 is considered and the responses of induction generators including synchronous generators under this condition are presented and discussed. The results

are compared with the conventional system. The base kV and base MVA is selected to be the same as the standard test system.

IV. REACTANCE DIAGRAM OF WSCC 9 BUS SYSTEM

The reactance diagram of WSCC 9 bus system under steady state condition is shown in the Figure 3. The resistances are neglected. The reactance diagram can be used for the system having induction generators by using exponentially varying reactance to calculate SC current of induction generators when they replaces the conventional Gs. Figure.4 indicates the equivalent circuit for 3 L-G fault at bus-5 for WSCC 9 bus system where the sub-transient reactance of synchronous generators are indicated at as X'' . The time taken by reactance to reach to infinite value depends up on machine parameters and fault location. This time is also different for different types of IGs. Due to the absence of damper winding, IGs does not undergo any sub transient period like SGs. Due to damper winding, the sub transient reactance of SGs is low, hence the peak value of short circuit current of SGs is higher as compared to IGs. The IGs enters the transient period after short-circuit occurrence, which is characterized by higher impedance as compared to the sub-transient impedance of the SG. The DC time constant of the SGs is lower compared to that of IGs. This is due to high inductance associated with the IGs resulted from inductive coupling between the stator and rotor circuit. The AC time constant in SGs and IGs are almost the same. Finally, the steady-state current of SGs is much higher than the steady-state current of the IGs as internal impedance of the IGs is higher. The high DC time constant and low steady-state current of the IGs lead to delayed zero crossing of the IGs short circuit current. This delay will cause the delay in the operation of the protective devices and create difficulty in finding proper settings for the protection relays.

V. SIMULATION RESULTS

For the proposed work, initially WSCC 9-bus system is simulated considering all the synchronous generators using PSCAD-EMTDC. The 3 L-G fault is simulated for 0.083 sec (4 cycle) at 10 sec at bus 5. The power flow and voltage at various buses for system loads were established under the steady state (base case) for all cases. The instantaneous current, Active power, Reactive power and RMS voltage is presented for the pre-fault, during-fault and post-fault duration.

Performance Evaluation of Wind Turbine Generators under System Fault Conditions in a Multi-Machine Power System

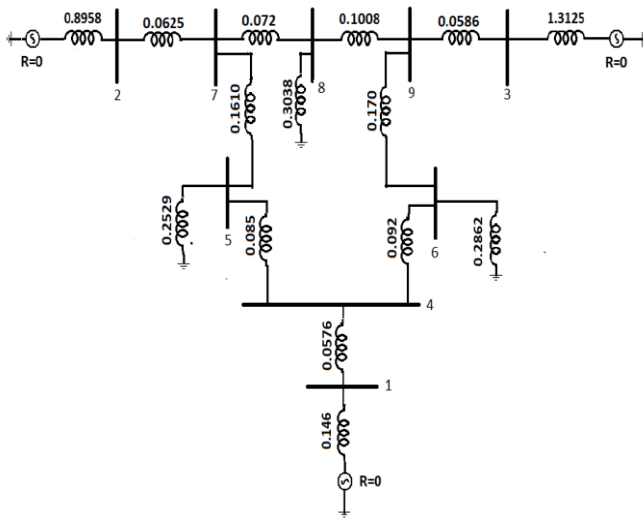


Figure 3: Reactance Diagram of WSCC 9 bus system under steady state condition. All values are in pu.

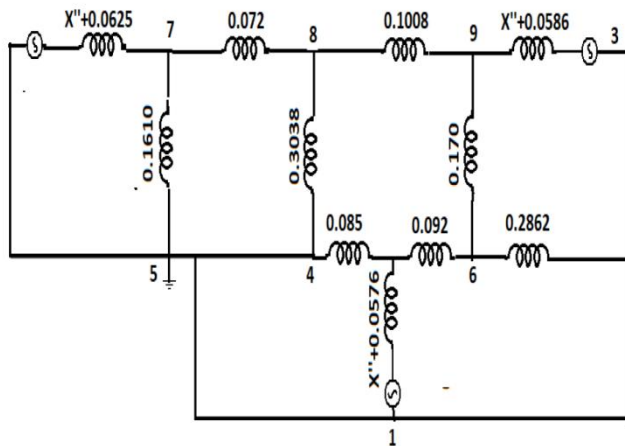


Figure 4: Equivalent circuit of WSCC 9 bus system after considering 3L-G fault at bus 5

A. Case-I – Symmetrical (3L-G) fault at bus 5 in conventional WSCC 9 bus system

Initially the base case is considered and the results of instantaneous currents, active power, reactive power, RMS voltage of all the three synchronous generators are depicted in Figure 5, 6, 7 and 8 respectively. These results are considered as the base to identify the effects of various induction generators technologies when they replace synchronous generator at bus 2.

B. Case-II – Symmetrical (3L-G) fault at bus 5 in modified WSCC 9 bus system with fixed speed induction generators (FSIG) based wind farm

It would be interesting to understand the effects of the system fault on the behaviour of synchronous generators in the presence of the largely penetrating induction generators (wind farm at bus 2). The SG at bus 2 in conventional WSCC 9 bus system is replaced by FSIG based wind farm. The wind farm has the same active power generation capacity as the SGs under the steady state condition.

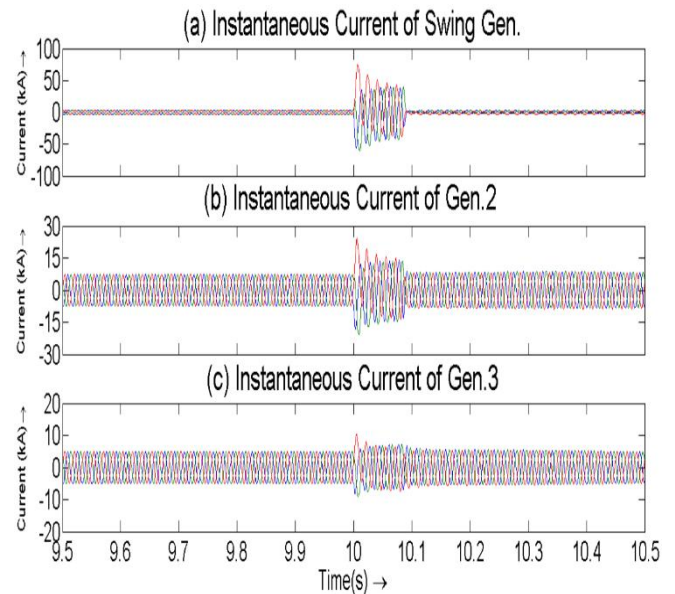


Figure 5: Three-phase instantaneous current of all the generators in a WSCC 3-generator 9-bus system, in pre-fault, during fault and post fault condition

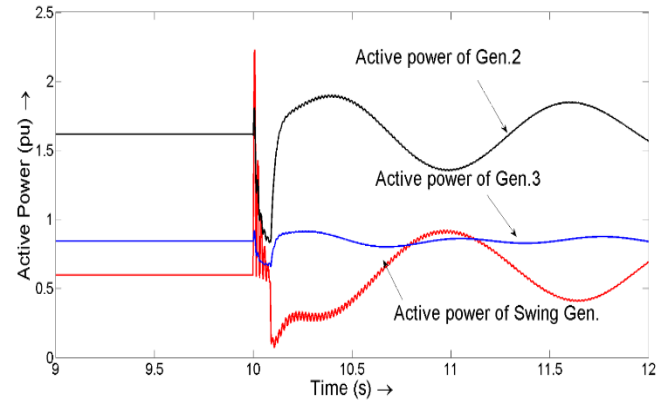


Figure 6: Active power (pu) of three generators in WSCC 3 generator 9- bus system in pre- fault, during fault and post fault condition

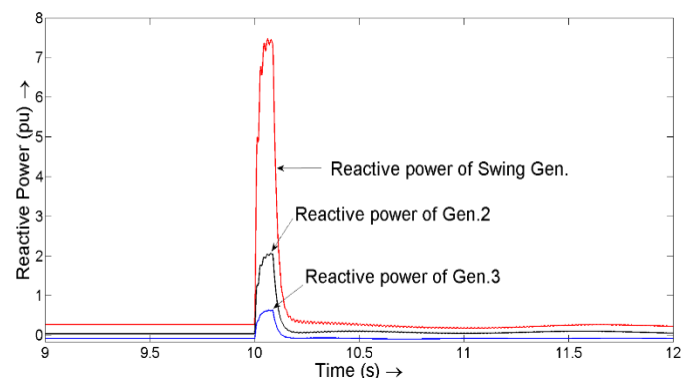


Figure 7: Reactive power (pu) of three generators in WSCC 3-generator 9-bus system in pre- fault, during fault and post fault condition

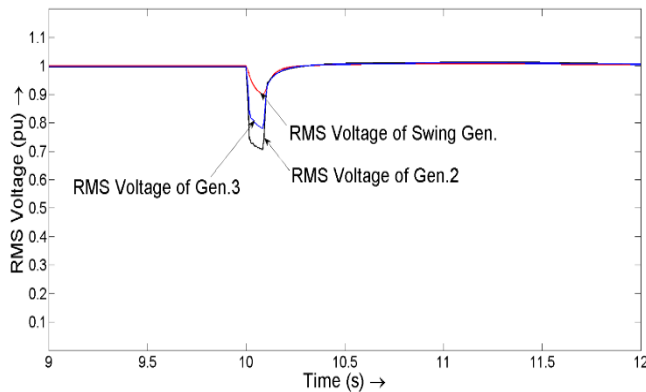


Figure 8: RMS Voltage (pu) of three generators in WSCC 3-generator 9-bus system in pre-fault, during fault and post fault condition

The relevant measurements are obtained at appropriate buses. The results of instantaneous currents, active power, reactive power, RMS voltage of all the three generators are depicted in Figure 9, 10, 11 and 12 respectively during pre-fault, fault and post-fault conditions. It is observed that symmetrical fault at bus 5 does not demand a large fault current from the induction generator as the systems impedance plays its role and inability of IGs to deliver reactive power during voltage sag. The peak fault current from the FSIG is reaching to just 2 pu (as against 5pu in case of terminal fault) [6] and its oscillations are reduced. The contribution to the fault current from both the synchronous generators do not significantly vary (except momentarily) however the magnitude of the current of swing generator rises and hence the active powers (Figure 10). The system regains the stable condition, as the fault is cleared in 0.083 s (4 cycles in 60Hz system). It is required to see that the reactive power demanded from the generators (especially swing generator) is quite significant under this condition (Figure 11). Under the fault at bus 5, the generator bus RMS Voltages falls to 0.52 pu, (Figure 12) much above the low voltage ride through (LVRT) requirements and system will continue to operate until the fault is cleared. Here, as capacitor connected with induction generator discharges, voltage gradually decreasing to absorb more reactive power from system. If fault duration is large and IG starts absorbing reactive power from system as the capacitor gets discharged it worsens voltage profile of system. After clearance of fault, capacitor again takes large inrush current. This scenario demands huge current drawn by system and it will be provided by the other SGs in the system hence, it prevents synchronization of generators with the grid. It shows the dependence of voltage stability with transient stability in the system with higher penetration of IGs. For change in the capacitance value, there will be a significant change in performance of FSIG at time of fault. The same effect is present for WRIG generators. However, value of capacitor bank (in WRIG only) is very less as compared to FSIG. Hence, it demands less inrush current from system. There is no need for capacitor bank for DFIG.

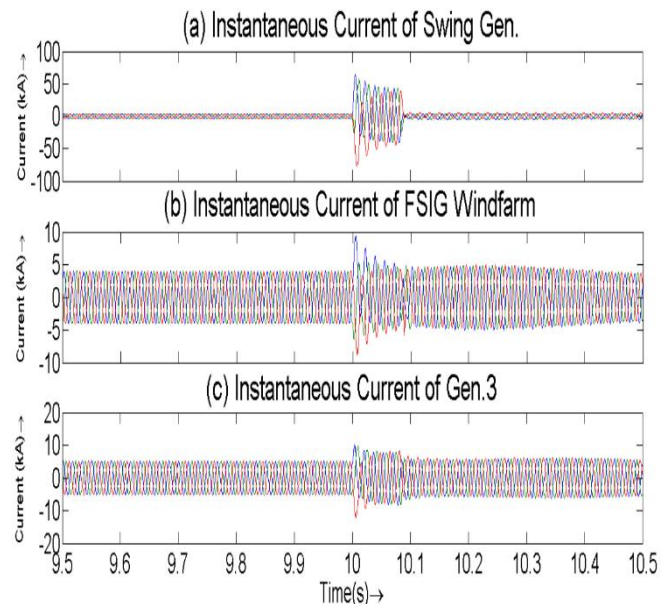


Figure 9: Three-phase instantaneous current of all the generators in a modified WSCC 3-generator 9-bus system, where synchronous gen.2 is replaced with equally rated FSIG based wind farm in pre-fault, during fault and post fault condition

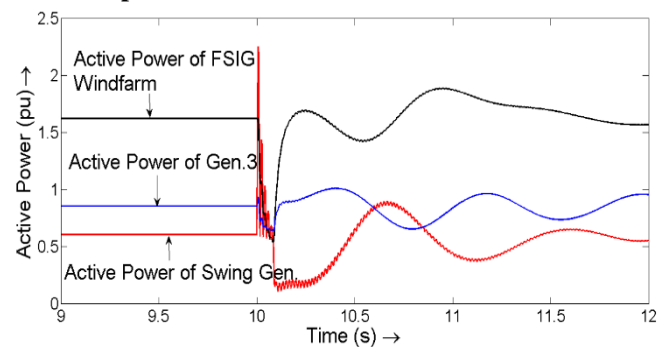


Figure 10: Active power (pu) of three generators in modified WSCC 3-generator 9-bus system where synchronous gen.2 is replaced with equally rated FSIG based wind farm in pre-fault, during fault and post fault condition

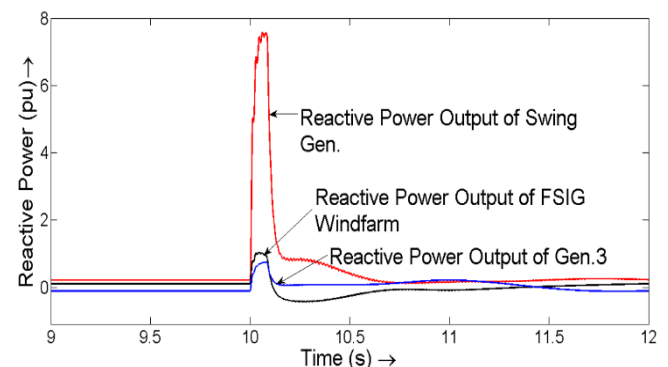


Figure 11: Reactive power (pu) of three generators in modified WSCC 3-generator 9-bus system where synchronous gen.2 is replaced with equally rated FSIG based wind farm in pre-fault, during fault and post fault condition

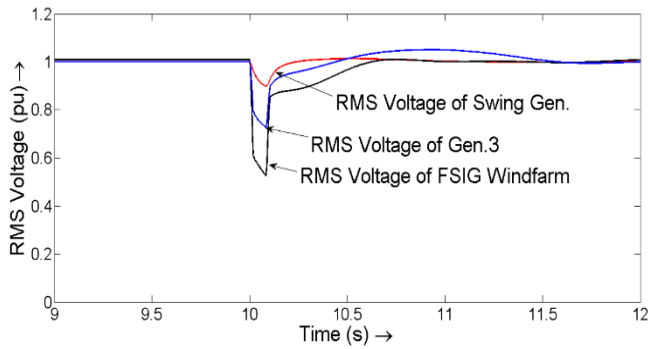


Figure 12: RMS Voltage (pu) of three generators in modified WSCC 3-generator 9-bus system where synchronous gen.2 is replaced with equally rated FSIG based wind farm in pre- fault, during fault and post fault condition

C. Case-III – Symmetrical (3L-G) fault at bus 5 in modified WSCC 9 bus system with wound rotor induction generators (WRIG) based wind farm

The performance of WRIG under the fault is better as compared to Type I, due to slip-ring based rotor resistance control. The short circuit fault current (due to fault at bus 5) in generator phases is significantly reduced (Figure 13) as compared to that in FSIGs. The RMS voltage of the wind-farm falls to nearly 0.1239 pu (Figure 16) which is quite significantly lower as compared to FSIG based wind farm due to the effect of capacitor bank. It is observed that system impedance plays the role in maintaining the generator voltages and power during the severe faults other than the generator terminal faults.

D. Case-IV – Symmetrical (3L-G) fault at bus 5 in modified WSCC 9 bus system with doubly fed induction generators (DFIG) based wind farm

In this case as the fault is at far distance, the voltage at DFIG terminal will not reduce to zero hence the crowbar will operate for initial cycles depending on the generator control. After removal of crowbar, the generator will contribute current (Figure 17) and it will provide reactive support to grid voltage. It is to be observed that under fault at bus 5, DFIG power delivery is affected to an extent (Figure 18) and the swing generator is forced to supply the load demand. Subsequent to clearance of fault, the voltage at the bus 2 starts building up, increasing the load current to steady state. The reactive power is demanded from the swing generator to a large magnitude (Figure 19). The RMS voltage of DFIG based wind farm is reduced to nearly 0.3891 pu (Figure 20) as the converter circuits capacitor will play its role and the RMS voltage does not fall to the level of WRIG based wind farms.

VI. RESULTS, COMPARISON AND DISCUSSION

As seen in Table-1 the RMS voltage of Generator 2 varies from 0.707 pu (Conventional WSCC system) to as low as 0.1239 pu (as in case of WRIG based wind farm). Also the conventional synchronous generator generates high amount of reactive power in case of fault which ultimately supports the voltage profile of the system unlike the cases of the wind farms.

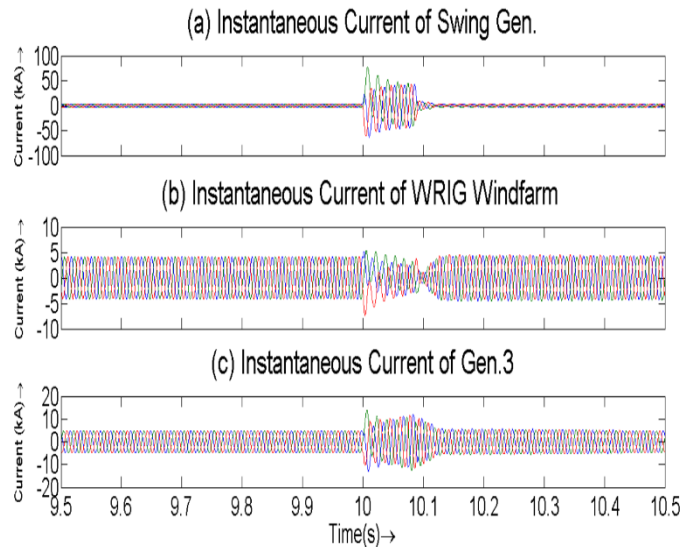


Figure 13: Three-phase instantaneous current of all the generators in a modified WSCC 3-generator 9-bus system, where synchronous gen.2 is replaced with equally rated WRIG based wind farm in pre- fault, during fault and post fault condition

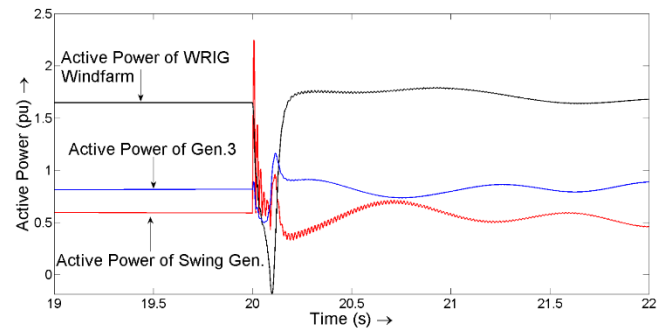


Figure 14: Active power (pu) of three generators in modified WSCC 3-generator 9-bus system where synchronous gen.2 is replaced with equally rated WRIG based wind farm in pre- fault, during fault and post fault condition

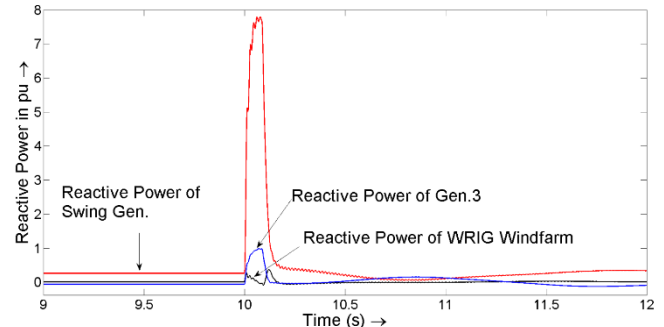


Figure 15: Reactive power (pu) of three generators in modified WSCC 3-generator 9-bus system where synchronous gen.2 is replaced with equally rated WRIG based wind farm in pre-fault, during fault and post fault condition

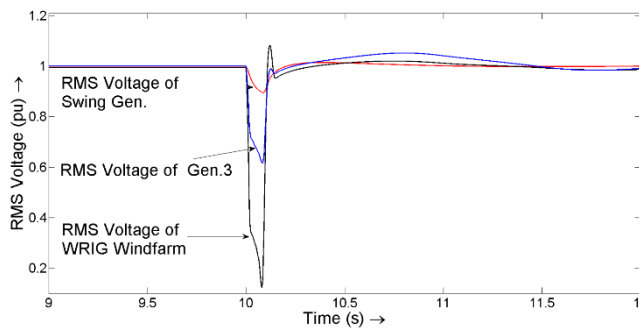


Figure 16: RMS Voltage (pu) of three generators in modified WSCC 3-generator 9-bus system where synchronous gen.2 is replaced with equally rated WRIG based wind farm in pre-fault, during fault and post fault condition

The induction generator cannot supply this high amount of reactive power as they do not have continuous flux provided by external excitation system. The reactive power management becomes critical for transient stability of the system. When SG is replaced by induction generators with its equivalent rating, the short circuit current contribution of both generators differs with respect to peak value and envelope. The peak value of Generator-2 changes from 24.10 kA to as low as 7.41 kA as shown in Table-2. It is to be noted that change in current envelope of induction generators brings change in current envelope of two other SGs in the case of discussion.

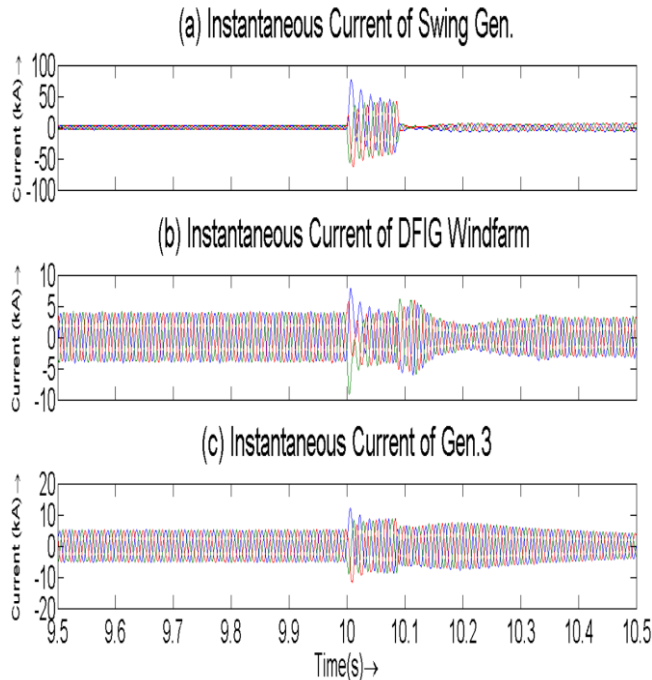


Figure 17: Three-phase instantaneous current of all the generators in a modified WSCC 3-generator 9-bus system, where synchronous gen.2 is replaced with equally rated DFIG based wind farm in pre- fault, during fault and post fault condition

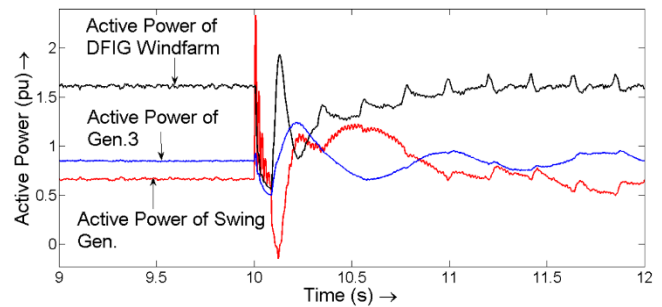


Figure 18: Active power (pu) of three generators in modified WSCC 3-generator 9-bus system where synchronous gen.2 is replaced with equally rated DFIG based wind farm in pre-fault, during fault and post fault condition

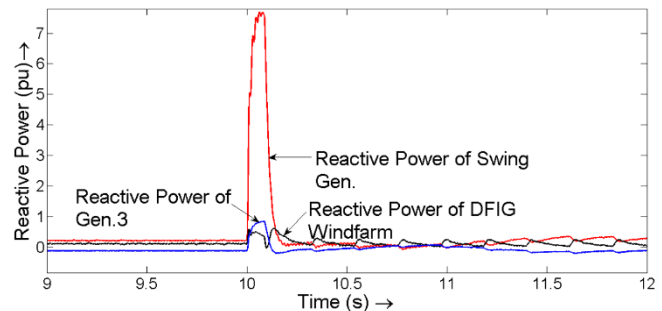


Figure 19: Reactive power (pu) of three generators in modified WSCC 3-generator 9-bus system where synchronous gen.2 is replaced with equally rated DFIG based wind farm in pre- fault, during fault and post fault condition

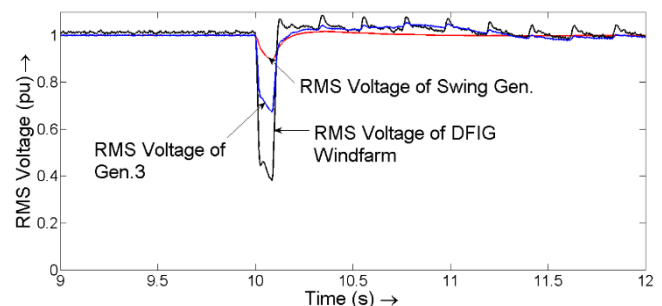


Figure 20: RMS Voltage (pu) of three generators in modified WSCC 3-generator 9-bus system where synchronous gen.2 is replaced with equally rated DFIG based wind farm in pre- fault, during fault and post fault condition

The current envelop in case of SG does not drop to zero while the current envelop of IGs drops to zero very fast specially in case of WRIG based wind farm (Figure 13). Hence, it demands change in relay setting and circuit breakers operation. Here, breaking energy dissipation of circuit breaker is same as energy dissipation during make operation. The induction generator(s) cannot supply requisite active power at the time of fault so the extra generation has to be compensated by swing and synchronous generator(s). Such changes affect operation of impedance relays especially and relay co-ordination.

Table-1: RMS voltage comparison for all cases (pu)

	Case-I	Case-II	Case-III	Case-IV
Generator 1	0.9010	0.8986	0.8958	0.8972
Generator 2	0.7070	0.5264	0.1239	0.3891
Generator 3	0.7817	0.7278	0.6190	0.6788

Table-2: Peak Short Circuit Current for all cases (kA)

	Case-I	Case-II	Case-III	Case-IV
Generator 1	74.68	75.79	77.19	76.07
Generator 2	24.10	9.45	7.41	9.21
Generator 3	10.43	11.93	14.07	12.17

VII. CONCLUSION

The paper shows the behaviour of various types of induction generator based wind farms with synchronous generators under the symmetrical fault at system level on one of the weak buses in a multi-machine power system. The analysis is very useful as the penetration of the renewable energy generation through wind energy is increasing day by day and it will help the power system operators to decide the ratings of circuit breakers under the system level fault. It is observed that the fault location has an impact on the short circuit current contributions by these generators, as the prior affects the voltage at each generator bus. If voltage across FSIG based wind farm fails to build up, it is not possible for system to regain its stability. In the present case, FSIG based wind farm is equipped with a large terminal capacitance, which discharges high current at the time of fault. The discharge rate of capacitor decides the transient stability margin in case of FSIG based wind farm. For WRIG based wind farm the peak current drops significantly due to the addition of rotor resistance and the RMS voltage also dips to very low value because of the absence of capacitors. The controllers and converters in DFIG wind farm, reduces the criticality of this issue as compared to FSIG based wind farm. So, to replace equivalent capacity by induction machines or addition of such generation, demands for the change in protection relay schemes, preferably the adaptive ones.

REFERENCES

1. A. K. Elnaggar, J. L. Rueda, and I. Erlich, "Comparison of short-circuit current contribution of Doubly-Fed induction generator based wind turbines and synchronous generator," IEEE Grenoble Conference, Grenoble, France, 2013, pp. 1–6.
2. R. E. Doherty, E. T. Williamson, "Short-Circuit Current of Induction Motors and Generators," Journal of the American Institute of Electrical Engineers, 1921, Vol. 40, Issue: 1.
3. J. Martinez, P. C. Kjar, P. Rodriguez, and R. Teodorescu, "Short circuit signatures from different wind turbine generator types," IEEE/PES Power Systems Conference and Exposition, Phoenix, AZ, USA, 2011, pp. 1–7.
4. F. Sulla, J. Svensson, and O. Samuelsson, "Fault behavior of wind farms with fixed-speed and Doubly-Fed Induction Generators," IEEE Trondheim Power Tech, Trondheim, 2011, pp. 1–7.
5. E. Muljadi, N. Samaan, V. Gevorgian, J. Li, and S. Pasupulati, "Different Factors Affecting Short Circuit Behavior of a Wind Power Plant," IEEE Transactions on Industry Applications, vol. 49, no. 1, pp. 284–292, Jan.2013.

6. V. Gevorgian, M. Singh and E. Muljadi, "Symmetrical and unsymmetrical fault currents of a wind power plant," IEEE Power and Energy Society General Meeting, San Diego, CA, 2012, pp. 1–8.
7. E. Muljadi and V. Gevorgian, "Short-circuit modeling of a wind power plant," IEEE Power and Energy Society General Meeting, Detroit, MI, USA, 2011, pp. 1–9.
8. J. Morren and S. W. H. de Haan, "Short-Circuit Current of Wind Turbines With Doubly Fed Induction Generator," IEEE Transactions on Energy Conversion, vol. 22, no. 1, pp. 174–180, Mar. 2007.
9. A. El-Naggar and I. Erlich, "Analysis of fault current contribution of Doubly-Fed Induction Generator Wind Turbines during unbalanced grid faults," Renewable Energy, vol. 91, pp. 137–146, Jun. 2016.
10. S. Das and S. Santoso, "Effect of wind speed variation on the short-circuit contribution of a wind turbine," IEEE Power and Energy Society General Meeting, San Diego, CA, 2012, pp. 1–8.
11. Ahmed El-Naggar, Istavan Erlich, "Fault current contribution analysis of doubly fed induction generator based wind turbines," IEEE transaction on energy conversion, Vol 30 No 3 Sep 2015.
12. T. Sun, Z. Chen, F. Blaabjerg "Voltage recovery of grid-connected wind turbines with DFIG after a short circuit fault," IEEE 35th annual power electronics specialists conference, 2004
13. T. Kauffmann U. Karaagac, I. Kocar, S. Jensen, J. Mahseredijan and E. Farantatos, "An accurate type III wind turbine generator short circuit model for protection applications", IEEE transactions on power delivery, Vol 32, No 6, pp 230-2379 Dec 2017.
14. J. Ouyang, D. Zheng, X. Xiong, C. Xiao, and R. Yu, "Short-circuit current of doubly fed induction generator under partial and asymmetrical voltage drop," Renewable Energy, vol. 88, pp. 1–11, Apr. 2016.
15. E. Muljadi, C. P. Butterfield, B. Parsons, and A. Ellis, "Effect of Variable Speed Wind Turbine Generator on Stability of a Weak Grid," IEEE Transactions on Energy Conversion, vol. 22, no. 1, pp. 29–36, Mar. 2007.
16. Vishnuvardhan Telukunta, Janmejaya Pradhan, Anubha Agrawal, Manohar Singh, Sankighatta Garudachar Sri vani, "protection challenges under bulk penetration of renewable energy resources in power systems: A review," CSEE Journal of Power and Energy Systems, vol. 3, no.4, pp. 365–379, Dec. 2017.
17. Sachin Srivastava, Abhinna Chandra Biswal, Sethuraman Ganesan, U. J. Shenoy, "Impedance seen by Distance Relays on Lines Fed from Fixed Speed Wind Turbines", International Journal of Emerging Electric Power Systems, Vol. 14, Issue 1, 201
18. S. Srivastava, U. J. Shenoy, A. C. Biswal, and S. Ganesan, "Effect of fault resistance and grid short circuit MVA on impedance seen by distance relays on lines fed from wind turbine generating units (WTGU)," 11th IET Inter-national Conference on Developments in Power Systems Protection (DPSP 2012), Birmingham, UK, 2012.
19. L. Simon and K. S. Swarup, "Impact of DFIG based wind energy conversion system on fault studies and power swings," in 2016 National Power Systems Conference (NPSC), Bhubaneswar, India, 2016, pp. 1–6.
20. P.M. Anderson and A. A. Fouad, "Power System Control and Stability, Iowa State University Press," Ames, IA, 1977

Table-3: Rating of wind turbine generators

Generator Type	FSIG	DFIG - WRIG
Rated Power (MVA)	5	5
Rated Voltage (kV)	0.69	0.69
Inertia Constant (sec.)	4.32	3
Stator Resistance (pu)	0.0054	0.0054
Wound rotor Resistance (pu)	0.00607	0.00607
Magnetizing inductance (pu)	4.5	4.5
Stator leakage inductance (pu)	0.1	0.1
Wound rotor leakage inductance (pu)	0.11	0.11

AUTHORS PROFILE



Chintan R. Mehta is currently working as Assistant Professor in Electrical Engineering Department at Institute of Technology, Nirma University, Ahmedabad. He has obtained M.E. in Electrical Engineering from Gujarat University. He has many research publication to his credit.



Urmil B. Bhatt has obtained M. Tech in Electrical Power Systems from Nirma University.



Dishang D. Trivedi obtained Ph.D. from Nirma University. He is at present working as Associate Professor in L. D. College of Engineering. He has many research publications to his credit.



Santosh C. Vora is working as Head of Electrical Engineering Department at Institute of Technology, Nirma University. He has obtained Ph.D. from Indian Institute of Science, Bangalaoe. He has many research publications to his credit in international and national journals & conferences.